HIF-1α is neuroprotective during the early phases of mild hypoxia

Beatriz López-Hernández[1,2], Inmaculada Posadas[1,2], Petar Podlesniy[2,3], Maria A. Abad [2,3], Ramon Trullas[2,3]. and Valentín Ceña[1,2,3].

[1]Unidad Asociada Neurodeath, Facultad de Medicina, Universidad de Castilla-La Mancha. Albacete, Spain; [2]CIBERNED, Instituto de Salud Carlos III, Spain and 3 Neurobiology Unit, Institut d'Investigacions Biomèdiques de Barcelona, CSIC/IDIBAPS, 08036 Barcelona, Spain.

Number of pages:
Number of words in Abstract.
Number of words in Introduction:
Number of words in Discussion:

[3]Address correspondence to:

Prof. Valentín Ceña
Unidad Asociada Neurodeath
Facultad de Medicina
Avda. Almansa, 14
02006 Albacete (SPAIN)
Email: valentin.cena@gmail.com
Telephone +34680222322
FAX +34967599316

Acknowledgements: We thank Elena Galera for her technical assistance. This work has been supported, in part, by the Programa Ramón y Cajal from Ministerio de Educación y Ciencia (Spain) and UCLM-CCM to IP, grants PAI07-0063 and PI-2007/47 from JCCM to IP, SAF2008-03514 to RT and grants PI081434 from Fondo de Investigaciones Sanitarias, BFU2011-30161-C02-01 from Ministerio de Ciencia e Innovación and PII1I09-0163-4002 and POII10-0274-3182 from Consejería de Educación, JCCM to VC.

Abstract

Hypoxia-inducible factor 1α (HIF-1α) is a transcription factor that plays a key role regulating the adaptive response to hypoxia. HIF-1α is stabilised during hypoxia and, after dimerization with HIF-1β, triggers the expression of different genes involved in cell cycle control and energy metabolism associated with cell survival. However, HIF-1α also regulates the expression of pro-apoptotic genes. The aim of this work is to ascertain the influence of HIF-1α on neurotoxicity evoked by hypoxia in rat cortical neurons. We found that mild hypoxia induces a time-dependent neuronal death that involves free radical production, mitochondrial depolarization, cytochrome c release and caspase 3 activation. Lentiviral mediated knockdown of HIF-1α markedly potentiated all these effects during the initial 24 hours of hypoxia suggesting that HIF-1α plays a neuroprotective role on hypoxia-mediated neuronal death. After this period, the protective actions of HIF-1α disappeared in agreement with the time-course of hypoxia-mediated HIF-1α stabilization. On the other hand, lentiviral mediated over expression of HIF-1α increased lactate dehydrogenase A, one of the target genes for HIF-1α, but did not show protective actions on hypoxia-mediated neuronal death indicating that the level of endogenous HIF-1α stabilization achieved during hypoxia is already the maximal required for the transcription activities of HIF-1α. These results indicate that HIF-1α is neuroprotective in the early phases of hypoxia.

Introduction

Hypoxia inducible factor 1α (HIF-1α), a transcription factor that is stabilized and activated by hypoxia, has been described as a master regulator of the cellular response to low oxygen tension. Under normoxia, HIF-1α is continuously synthesized and its protein levels and transcriptional activity are finely regulated by different mechanisms (Ratcliffe et al., 1998). The most important regulatory system is proteolysis by different oxygen-dependent mechanisms including hydroxylation by prolyl-hydroxylases (Semenza et al., 2000;Stolze et al., 2006) that allows its ubiquitination and proteosomal degradation (Cockman et al., 2000). Once HIF-1α protein is stabilized, it dimerizes with the constitutively expressed HIF-1β subunit, leading to its translocation to the nucleus where it switches on a series of genes participating in compensatory mechanisms including regulation of angiogenesis (Forsythe et al., 1996), vasomotor control (Palmer et al., 1998), erythropoiesis (Wang and Semenza, 1993), iron metabolism (Mukhopadhyay et al., 2000), cell cycle control (Carmeliet et al., 1998) and energy metabolism (Ebert et al., 1995).

Paradoxically, HIF-1α has also been related to hypoxia-dependent apoptosis (Carmeliet et al., 1998;Wood and Youle, 1995). While HIF-1α dependent genes participating in the adaptive response to hypoxia are widely characterized, genes mediating its proapoptotic function remain largely unknown. Some of the genes identified include *Nip3*, a proapoptotic member of the Bcl-2 proapoptotic family (Sowter et al., 2001), the stress response gene *RTP801* (Shoshani et al., 2002) or the type II nitric oxide synthase (Palmer et al., 1998). In addition, HIF-1α might act as a pro-apoptotic factor through its binding to p53 tumor suppressor protein which is able to increase the expression of target genes coding for pro-apoptotic proteins like Bax (An et al., 1998).

During an ischemic insult, HIF-1α levels decrease gradually from the ischemic core to more distant regions (Demougeot et al., 2004) indicating that induction and expression of HIF-1α in ischemic areas is heterogeneous. Moreover, both neuroprotective and detrimental effects of HIF-1α have been observed in different models of ischemia (Halterman et al., 1999;Siddiq et al., 2005;Helton et al., 2005;Baranova et al., 2007). These controversial data might suggest that HIF-1α is involved in the cell response to ischemia with a dual effect depending on the severity of the insult. This dual effect makes important to establish if HIF-1α plays a neuroprotective or detrimental role on neurons during hypoxia and the molecular mechanisms involved in its actions. Ultimately, a better understanding of these processes might help to find new pharmacological targets to treat brain ischemia.

To elucidate whether HIF-1α plays a protective or detrimental role during mild hypoxia-mediated neuronal death, we studied the effect of lentiviral mediated over expression and knockdown HIF-1α and found that HIF-1α protects neurons from apoptosis under mild hypoxia for the first 24 hours. However, under prolonged hypoxia this neuroprotective effect is surpassed by the insult and the neurons eventually die by apoptosis.

Material and Methods

Cell culture.

Primary cultures of brain cortical neurons were essentially prepared as described previously (Posadas et al., 2010). The frontal–lateral cortical lobes were dissected out of Sprague Dawley embryonic day 17 rat fetuses, and the cells were chemically dissociated in the presence of trypsin and DNAase I. After isolation cells were resuspended in serum free Neurobasal medium supplemented with B27 containing 2 mM L-glutamine, penicilin (20 U/ml) and streptomycin (5µg/ml), and plated on poly-L-lysine-coated 24- or 6-well plates or on poly-L-lysine-coated glass coverslips. Cortical cells were maintained at 37°C in a saturated humidity atmosphere cointaining 95% air and 5% CO_2 and used for experiments after 7-12 days in vitro (DIV). All animals were treated and sacrificed in accordance with guidelines of the European Union (86/609/EEC) for the use of laboratory animals.

Lentiviral vectors preparation.

The self-inactivating bicistronic lentiviral transfer vector constructs pWPI and pLVTHM, as well as the second-generation lentivirus packaging and envelope plasmids, were obtained from Addgene (Cambrigde, MA). The map and the sequences of these plasmids are available at Addgene (http://www.addgene.org/). The coding sequence for HIF-1α was cloned from rat brain cDNA (Quick Clone cDNA; Invitrogen) by PCR. The pWPI-HIF-1α-GFP vector was obtained by inserting the HIF-1α cDNA by blunt end ligation into pWPI using the PmeI restriction sites. The vector pLVTHM-shRNAi-HIF-1α-GFP was constructed to express short interfering RNAs to silence HIF-1α expression. A sequence targeting HIF-1α was selected based on the rules for RNAi susceptibility proposed by Tuschl's group

(Elbashir et al., 2001) and using the RNAi prediction program from the Bioinformatics group of the Whitehead Institute for Biomedical Research. Two complementary DNA oligonucleotides (Roche, Berlin, Germany) were annealed to produce a double stranded DNA fragment encoding a 19-nucleotide sense strand, 9-nucleotide loop, and 19-nucleotide antisense strand of the HIF-1α target or of a random sequence. The sequence of the HIF-1α shRNAi was as follows:5'-cgcgtccccGAGCTCCCATCTTGATAAATtcaagagaTTTATCAAGATGGGAGCTCttttt ggaaat-3'(sense) and 5'-cgatttccAAAAAGAGCTCCCATCTTGATAAAtctcttAGGGAGCTCgggga-3' (antisense). The sequence in capitals is the HIF-1α target sequence that corresponds to bases 176-194 of the HIF-1α mRNA (GenBank accession number NM_023459). We also designed a shRNAi with a random sequence to use as a control lentivector. The sequence of the shRNAi-Random is as follows: 5'-gatccccGCAGTGCAATATCGGAAACttcaagagaGTTTCCGATA TTGCA-CTGCttttt-3' (sense) and 5'-agctaaaaaGCAGTGCAATATCGGAAACtctcttgaaGTTTCCGATATTG CACTGCggg-3' (antisense). The duplex DNAs of shRNAi-HIF-1α and shRNAi-Random were cloned into the *ClaI* and *MluI* sites of the pLVTHM vector. The viral particles pseudotyped with vesicular stomatitis virus G glycoprotein were produced by transient transfection in 293T cells plated in 100 mm dishes in DMEM plus 10% FBS. When subconfluent, 293T cells were cotransfected with 10 μg of lentiviral vector containing the transgene, 7.5 μg of the packaging plasmid psPAX2, and 3 μg of the envelope plasmid pMD2G, using the calcium phosphate transfection method. After 16 h, the medium was replaced, and the virus particles were harvested 24 h later by collecting the medium. High-titer stocks (3 x 10^6 transduction units per microliter) were obtained by ultracentrifugation and resuspension of the viral pellet in

TNE buffer (50 mM Tris-HCl, pH 7.5, 130 mM NaCl, and 1 mM EDTA). Viral stocks were stored at -20°C and used within 1 month.

Transduction of cortical neurons with lentiviral vectors.

Cortical neurons were plated on poly-L-lysine-coated glass coverslips and immediately after plating different volumes of viral stocks were added. After 24 hours, the medium was replaced and at 48 hours post-infection, cells were washed with PBS and GFP fluorescence was observed using an excitation filter of 490 nm and an emission filter of 520 nm in a Nikon Diaphot inverted microscope equipped with a 75W Xenon lamp and a Nikon 40X, 1.3 numerical aperture, epifluorescence oil immersion objective. Transfection efficiency was calculated by counting the number of fluorescein-positive cells over total number of cells in 9 randomly selected regions from three independent experiments.

Hypoxia paradigm.

Cortical neurons were plated on poly-L-lysine-coated 24- or 6-well plates or on poly-L-lysine-coated glass coverslips. At DIV 7-12, cells were exposed to normoxia (Nx): saturated humidity atmosphere cointaining 95% air and 5% CO_2; or hypoxia (Hx): saturated humidity atmosphere cointaining 3% O_2 (which is equivalent to a pO_2 of 22.8 mm Hg which is slightly lower than the PO_2 of the blood in the venous compartment) 5% CO_2, and balanced N_2, at 37°C. Hypoxic conditions were generated in a Heracell® 150 incubator (Kendro laboratory Products GmbH).

MTT Assay:

MTT assay was preformed as previously described (Posadas et al., 2007). Briefly, cortical neurons were plated on poly-L-lysine-coated 24-well plates and transduced

or not with the indicated lentiviral vector. At DIV 7-12, neurons were exposed to normoxic or hypoxic conditions for different periods of time. Afterwards, MTT (5 mg/ml) was added to each well (10% total volume), and the cells were incubated at 37°C for 3 h. Then, culture medium was removed and the insoluble formazan crystals were dissolved in 300 µl DMSO (Merck), aliquots of 50 µl were transferred to a 96-well microplate and measured spectrophotometrically in an ELISA reader (Microplate Reader 2001, Bio-Whittaker) at 590 nm.

Hoescht 33342 Staining.

Cortical neurons were plated on poly-L-lysine-coated glass coverslips (20 mm). At DIV 7-12, cells were exposed to normoxia or hypoxia for different times. After incubation period, cells were loaded with 1 µM Hoescht 33342 for 5 min at 37°C in Krebs–Henseleit solution. Cells were then washed twice with Krebs–Henseleit solution and the fluorescence was observed using an excitation filter of 350 nm and an emission filter of 450 nm in a Nikon Diaphot inverted microscope equipped with a 75W Xenon lamp and a Nikon 40X, 1.3 numerical aperture, epifluorescence oil immersion objective. Images were acquired with a CCD camera and analyzed using commercial software (Universal Imaging; Molecular Devices; Toronto, Ontario, Canada).

Caspase 3 activity.

Cortical neurons were plated on poly-L-lysine-coated 6-well culture plates. After 7-12 DIV, neurons were exposed to normoxia or hypoxia for different times. In another set of experiments, cells were transduced with pVTHM-shRandom or pLVTHM-shHIF-1α after plating and incubated under normoxia or hypoxia. Afterwards, cells were washed twice with cold PBS and lysed in lysis buffer containing 100 mM *N*-2-

hydroxyethylpiperazine-*N*′-2-ethanesulphonic acid (HEPES), 5 mM dithiothreitol (DTT), 5 mM ethylene glycol-bis (*β*-aminoethyl ether)-*N*,*N*,*N*′,*N*′,-tetraacetic acid (EGTA), 0.04% Nonidet P-40 and 20% glycerol; pH 7.4. Extracts were then centrifuged at 5000 × *g* for 10 min at 4°C, and protein content was determined by using the bicinchoninic acid (BCA) protein assay according to the manufacturer's instructions (Pierce Biotechnology Inc.). Caspase 3 activity was determined as previously described using the fluorescence substrate Asp-Glu-Val-Asp-7-amino-4 trifluoromethyl-coumaryl (Z-DEVD-AFC) at 37°C (Jordan et al., 2000). Caspase 3 activity was expressed as times fold of basal activity detected in normoxia-treated neurons.

Total lysates.

Cortical neurons were plated on poly-L-lysine-coated 6-well culture plates. After 7-12 DIV, neurons were exposed to normoxia or hypoxia for different times. In another set of experiments, cells were previously transduced with each lentivirus after plating and at 7-12 DIV incubated under normoxia or hypoxia for 6h. Afterwards, cells were washed twice with cold PBS and resuspended in homogenization buffer containing 10 mM Hepes, 0.32 M sucrose, 100 µM EDTA, 1 mM DTT, 0.1 mM PMSF, 40 µg/ml aprotinine, 20 µg/ml leupeptine; pH 7.4. Neurons were homogenated using a polytron (two cycles, 10 s at maximum speed). Homogenates were then centrifuged at 5,000×g for 10 min at 4°C. The supernatants, i.e. total lysates, were removed and stored at -80ºC until analysed by gel electrophoresis.

Preparation of cytosolic and mitochondrial fractions.

Cortical neurons were plated on poly-L-lysine-coated 6-well culture plates. After 7-12 DIV, cells were exposed to normoxia or hypoxia for different times. In another set of

experiments, cells were transduced with pVTHM-shRandom or pLVTHM-shHIF-1α after plating and incubated under normoxia or hypoxia for 18h. Afterwards, cells were washed twice with PBS, scraped and collected by centrifugation at 1500 *xg* for 10 min. Cell pellets were resuspended in extraction buffer containing 250mM sucrose, 50mM Tris-HCl, 1mM EGTA, 2.5mM EDTA, 50 mM Na_3VO_4, 1mM DTT, 0.1mM PMSF, 40 µg/ml aprotinin, 20 µg/ml leupeptin; pH 7.4 and homogenized with a pellet pestle (Sigma, St Louis, MO, USA) (25 strokes) and, after 15 min on ice, centrifuged at 3000 xg for 5 min to remove cell nuclei and intact cells. Supernatants collected were then centrifuged at 20000 *xg* for 30 min at 4ºC. The supernatants, i.e. cytosolic fractions, were removed and stored at -80ºC until analysed by gel electrophoresis. Pellets containing mitochondria were resuspended in 50 µl of extraction buffer, homogenized with a pestle (5 strokes) and then centrifuged at 20,000 xg for 60 min at 4ºC. The supernatants, i.e., mitochondrial pellets, were removed and stored at -80ºC until analysed by gel electrophoresis.

Preparation of cytosolic and nuclear extracts.

Cortical neurons were plated on poly-L-lysine-coated 6-well plates, cultured for 7-12 DIV and then incubated under normoxia or hypoxia during different times. After these periods of incubation, cells were washed twice with ice-cold PBS, scraped and collected by centrifugation at 1,500 xg for 10 min. Cell pellets were resuspended in extraction buffer A containing (Hepes 10mM, EDTA 1mM, EGTA 1mM, KCl 10mM, DTT 1mM, FNa 5mM, Na_3VO_4 1mM, Leupeptin 1mg/ml, Aprotinin 0.1mg/ml, PMSF 0.5mM; pH 8). After 60 min on ice, Nonidet P-40 was added to reach a 0.5% concentration. Afterwards, the samples were gently vortexed for 15 s, and nuclei were sedimented by centrifugation at 20,000 xg for 30 s at 4 ºC. The supernatants, i.e. cytosolic extracts, were collected and stored at -80°C until analysed by gel

electrophoresis. Pellets were resuspended in 50 µl of Buffer B containing Hepes 20mM, EDTA 1mM, EGTA 1mM, NaCl 0.4M, DTT 1mM, FNa 5mM, Na_3VO_4 1mM, leupeptin 1mg/ml, aprotinin 0.1mg/ml, PMSF 0.5 mM; pH 8, and proteins were extracted by shaking samples for 30 min at 4ºC. Afterwards, samples were centrifuged at 20,000 xg for 15 min. The supernatants, i.e., nuclear extracts were collected and stored at -80°C until analysis by gel electrophoresis.

Western Blot Analysis.

Western blots were performed as previously described (Jordan et al., 2002). Protein samples from total lysates, mitochondrial, nuclear and cytosolic fractions (20 µg) were loaded on 10% or 15% PAGE-SDS and transferred onto nitrocellulose membranes. Membranes were blocked in PBS-Tween 20 (0.1%) containing 5% non-fat dry milk and 0.1% BSA for 1 h at 4°C and incubated with anti-HIF-1α monoclonal antibody (1:5,000) (RD System, Abingdon, England), anti-cytochrome *c* polyclonal antibody (1:1,000), anti-α-tubulin polyclonal antibody (1:2,000) (Calbiochem, Barcelona, Spain), anti-OxPhos Complex IV subunit IV monoclonal antibody (1:,1000) or anti-Histone H2A polyclonal antibody (1:1,000) (Cell Signaling, Beverly, MA) overnight at 4°C. Afterwards, blots were washed with PBS-Tween 20 (0.1%) and incubated with the appropriate Peroxidase conjugated (HRP)-antibody anti IgG (1:10,000) for 2 h at 4°C. Immunoreactive bands were visualized using an enhanced chemiluminiscence system (ECL; Amersham Biosciences). Densitometric analysis of immunoreactive bands was performed by using ImageQuant 5.2 software (Amersham Biosciences).

GSH measurement:

Cortical neurons were plated on 24-well plates and transduced or not with each lentivirus after plating. At DIV 7-12, cells were exposed to normoxia or hypoxia for different periods of time. Then, cells were washed twice with cold PBS and scraped in 1 ml of PBS. Cells collected were counted using a Neubauer chamber and after centrifugation at 1,500 ×g for 10 min, the pellet was resuspended in 5-sulphosalicylic acid (3.33%) containing 0.25 mM EDTA to prevent oxidation of GSH and to inhibit GSH-utilizing enzymes. Tubes were frozen and thawed three times to break the cells and release GSH. The lysate was then centrifuged (10,000 ×g for 5 min at 4°C) and the supernatant transferred to tubes kept in dry ice until assayed for GSH content. GSH measurements were performed as previously described (Posadas et al., 2010).

Mithochondrial transmembrane potential.

Cortical neurons were seeded on poly-L-lysine-coated glass coverslips, cultured for 7-12 DIV and exposed to normoxia or hypoxia for different times. In another set of experiments, cells were previously transduced or not with pLVTHM-shRandom or pLVTHM-shHIF-1α after plating for 18h. Mitochondrial transmembrane potential was determined as preiously described (Tornero et al., 2011). Briefly, cells were incubated in Krebs-Henseleit solution containing 10 μM Tetramehtyl-rhodamine-methyl-ester (TMRM) (Molecular Probes, Carlsbad, CA, USA) for 20 minutes at 37ºC, and then washed out. Fluorescence measurements were obtained using a Nikon Diaphot inverted microscope equipped with a 75 W Xenon lamp and a Nikon 40X, 1.3 numerical aperture, epifluorescence oil immersion objective. Fluorescence of TMRM was observed using an excitation filter of 535 nm and an emission filter of 590 nm. Afterwards, Krebs-Henseleit solution containing 10 μM carbonylcyanide p-trifluoromethoxyphenylhydrazone (FCCP) was added to each preparation to

dissipate the mitochondrial transmembrane potential (Ψ_m). Images were acquired every 15 seconds for 5 minutes with a CCD camera and analyzed using commercial software (Universal Imaging; Molecular Devices; Toronto, Ontario, Canada). Linear regression of fluorescence data were obtained for each experimental condition and the slopes of the lines fitted by least squares were taken as the rate of loss of mitochondrial transmembrane potential. The percentages of Ψm were calculated respect to data obtained under normoxia.

ROS measurement.

Cortical neurons were seeded on poly-L-lysine-coated glass coverslips (20mm). At DIV 7-12, cells were incubated under normoxic or hypoxic conditions for 6 to 24 h in Krebs-Henseleit solution containing the superoxide sensitive fluorescent dye MitoSox Red (2.5 μM; Invitrogen, Carlsbad, CA) for 30 min at 37ºC. Then, cells were washed and fixed with 4% p-formaldehyde for 20 min. Glass coverslips were mounted on slides, using Vectashield mounting medium (Vector Laboratories, Burlingame, California, USA). MitoSox fluorescence was observed using an excitation filter of 510 nm and an emission filter of 580 nm in a Nikon Diaphot inverted microscope equipped with a 75W Xenon lamp and a Nikon 40X, 1.3 numerical aperture, epifluorescence oil immersion objective. Images were acquired with a CCD camera and analyzed using commercial software (Universal Imaging; Molecular Devices; Toronto, Ontario, Canada).

Statistical analysis.

Data are expressed as mean ± SEM. Statistical analyses were carried out using the one-way analysis of variance and Bonferroni's *t*-test for multiple comparisons. Statistical results are given in the figure legends.

Results

Hypoxia induces apoptotic neuronal death

Cortical neurons were exposed to mild hypoxia (3% O_2) for different times and neuronal viability was determined using the MTT technique. LDH is a HIF-1α target gene which makes it unreliable as an index for toxicity under hypoxic conditions. Exposure of rat cortical neurons to reduced oxygen levels induced a time-dependent impairment of mitochondrial function (Fig. 1a). To confirm that the observed reduction in mitochondrial function following hypoxia was related to a loss in neuronal viability, we studied chromatin condensation and nuclei fragmentation, by Hoechst-33342 staining. We observed that exposure of cortical neurons to mild hypoxia produced a time-dependent increase in the number of nuclei with condensed or fragmented chromatin suggesting that mild hypoxia was inducing apoptosis in rat cortical neurons (fig 1b).

In addition, nuclei fragmentation was preceded by the release of cytochrome c from mitochondria to cytosol, which was initially detected at 6 h and maintained until 48 h (Fig. 1c), and subsequently by caspase 3 activation that was significantly increased at 18 h after hypoxia exposure, peaking at 48 h and decreasing thereafter (Fig. 1d). Taking together, these results indicate that moderate hypoxia induces cortical neuron apoptosis by activating the caspase-dependent intrinsic apoptotic pathway.

Hypoxia induces stabilization and translocation of HIF-1α to the nucleus

Next, we studied HIF-1α stabilization under mild hypoxia by exposing rat cortical neurons to hypoxia for different times. As it was expected, under normoxia conditions HIF-1α was undetectable, but when cortical neurons were exposed

to hypoxia HIF-1α was detected, in total cell lysates, as early as 3 h, reaching maximal levels of expression between 6 h and 24 h (Fig. 2a). It is interesting to note that HIF-1α expression decreased after 36 h, even if neurons were continuously exposed to mild hypoxia, being undetectable at 48 h (Fig. 2a). Since HIF-1α is a transcription factor, we explored whether there was also a translocation from cytosol to the nucleus. For this purpose, cortical neurons were incubated under hypoxia for different times, and cytosolic and nuclear fractions were obtained. Western blot analysis demonstrated that hypoxia not only promoted HIF-1α stabilization, but also promoted HIF-1α translocation from cytosol to nucleus as soon as 3 h after exposure to hypoxia (Fig. 2b, upper panel). The transcription factor was detected in nuclear fractions from 3 h to 18 h after hypoxia (Fig. 2b, lower panel). Densitometric analysis of HIF-1α expression in nuclear fraction demonstrated that maximal levels of this transcription factor were achieved at 3 h and maintained at least for 18 h (Fig. 2b, lower panel).

Mild hypoxia increases superoxide production and alters mitochondrial transmembrane potential

Since mitochondrial function impairment has been related to an increased production in reactive oxygen species (ROS) we decided to study the ROS levels in neurons exposed to mild hypoxia. Cells were exposed to normoxia and hypoxia for different times and superoxide production at mitochondrial level was studied by using the selective mitochondrial probe MitoSox. Cells were also stained with Hoechst-33342 to detect neuronal nucleus. Under normoxia, cortical neurons displayed a weak MitoSox fluorescence (Fig. 3a) indicating that low levels of superoxide anion are

produced by the mitochondrial transport chain. Exposure of cortical neurons to hypoxia induced a gradual increase of MitoSox fluorescence which was initially detected after 6 h and apparently peaked at 24 hours (Fig. 3a). It is important to note that after 6 h a punctuate pattern of the MitoSox probe, suggestive of a mitochondrial localization, could be observed indicating that superoxide anions were initially produced in mitochondria, whereas after 18 h of hypoxia MitoSox showed a diffuse staining which might suggest a change in the mitochondrial outer membrane permeability that allows diffusion of oxidized MitoSox from the mitochondria to cytosol. Moreover as it can be observed by nuclear Hoechst-33342 co-staining, the increased superoxide production correlated with neuronal apoptotic death that became evident between at 18 and 24 hours after exposure to hypoxia (Fig. 3a, right column). In accordance with the increase in superoxide anions production, sustained hypoxia caused a drastic reduction in neuronal gluthathione levels that was almost complete at 48 hours following ischemia (Fig. 3b). This drastic reduction in GSt levels detected after 24 hours may be a contributing factor to the neurotoxicity induced by reduced oxygen levels.

As seen in Fig. 3c, exposure of rat cortical neurons to mild hypoxia induced the collapse of the mitochondrial membrane potential (Ψm), which is considered a point of no return in the death cascade. This reduction in Ψm was evident after 6 h of hypoxia and reached about 50% following 24h of hypoxia (Fig. 3c). Interestingly, the time–course for the dissipation of Ψm is similar to the one for cytochrome c release from the mitochondria to cytosol (Fig. 2a). Moreover, hypoxia-generated superoxide anions might contribute to the hypoxia-mediated neuronal death because the cell-permeable superoxide dismutase (SOD) mimetic Mn-III tetrakis (4-benzoic acid) porphyrin chloride (MnTBAP) partially

prevents hypoxia-mediated death (Figure 3d). Taken together, our results suggest that mitochondrial superoxide overproduction plays a central role in mild hypoxia induced-neuronal apoptosis by inducing the mitochondrial permeability transition and allowing the liberation of proapoptotic factors such as cytochrome c.

Lentiviral-mediated RNAi delivery leads to efficient transduction and knockdown of HIF-1α in rat cortical neurons

To explore the role of HIF-1α in mild hypoxia-mediated neuronal death we used a loss of function approach by silencing HIF-1α expression using lentivirus-mediated transduction of a shRNAi against HIF-1α mRNA (pLVTHM-shHIF-1α). The green fluorescent protein (GFP) was used to examine lentivirus-transduction efficiency by microscopy. Cortical neurons were transduced with different volumes of viral stocks immediately after plating and, 48 h post-infection, fluorescence was observed. Microscopic images revealed high levels of lentiviral vector-mediated gene delivery and the transduction efficiency was calculated as percentage of GFP positive cells. Results showed that pLVTHM-shHIF-1α efficiently transduced cortical neurons achieving a transduction efficiency of 85-95% (Fig. 4a). This high efficiency correlated with high efficacy in reducing the target protein expression. Cortical neurons were transduced with pLVTHM-shHIF-1α and the effect on HIF-1α expression was studied under normoxia or after 6 h of exposure to mild hypoxia. Results showed that under hypoxia pLVTHM-shHIF-1α reduced endogenous HIF-1α protein levels efficiently, triggering a reduction of ~95% compared with the levels of HIF-1α stabilized in hypoxia-treated neurons (Fig. 4b), whilst a control pLVTHM-shRandom vector did not modify HIF-1α expression. Thus, lentiviral-mediated

shRNAi expression in cortical neurons selectively silenced HIF-1α expression under mild hypoxia.

Knockdown of HIF-1α increases hypoxia-induced neuronal death

Once determined that pLVTHM-shHIF-1α selectively prevents HIF-1α expression under hypoxia we explored whether HIF-1α was acting as a pro-survival or pro-death transcription factor under mild hypoxia in cortical neurons. Cells were transduced with pLVTHM-shHIF-1α or pLVTHM-shRandom and then exposed to normoxia or hypoxia for different times. Under normoxia, HIF-1α knockdown did not modify neuronal viability throughout the period of study (data not shown). However, transduction of rat cortical neurons with pLVTHM-shHIF-1α increased hypoxia-mediated collapse of Ψm (Fig. 5a), being the effect specific since transduction of rat cortical neurons with pLVTHM-shRandom did not modify the effect of hypoxia on Ψm (Fig. 5a). The drastic fall in Ψm detected in rat cortical neurons lacking HIF-1α and exposed to hypoxia for 18 h could be related to an increased ROS production at mitochondrial level that led to a greater mitochondrial permeability transition. As a result of this drastic reduction of Ψm a greater amount of cytochrome c release from mitochondria was detected in cortical neurons lacking HIF-1α and exposed to hypoxia (Fig. 5b) as well as a greater activity of caspase 3 in total lysates obtained from these cells (Fig. 5c).

Again, these effects on cytochrome c release and caspase 3 activation were specific of reduction of HIF-1α protein levels since pLVTHM-shRandom did not modify the effect of mild hypoxia on these parameters (Fig. 5b,c). Moreover, HIF-1α removal potentiates hypoxia-induced reduction in gluthathione levels, but only during the initial 24 hours (Fig. 5d). As a consequence of the above

effects, HIF-1α removal potentiates mild hypoxia-mediated neuronal death, but only during the initial 24 h of hypoxia (Fig. 5e) indicating that the lack of HIF-1α potentiates hypoxia induced-mitochondrial function impairment. It is interesting to note that this effect was sequence-specific because this phenomenon was not observed in cortical neurons transduced with pLVTHM-shRandom (Fig. 5e). These findings suggest that HIF-1α acts preventing the apoptotic neuronal death and support a neuroprotective role of this transcription factor in rat cortical neurons under the first 24 h of mild hypoxia.

Effect of HIF-1α over-expression on neuronal viability

Once established that HIF-1α plays a neuroprotective action during mild hypoxia, we attempted to protect cortical neurons from mild hypoxia by over expressing HIF-1α. For this purpose, cells were transduced with the control pWPI-empty vector or with pWPI-HIF-1α that encodes for HIF-1α protein. Both lentiviral vectors also contain the information to express GFP protein that was used to examine lentivirus-transduction efficiency by fluorescence microscopy. Cortical neurons were transduced with different volumes of viral stocks immediately after plating and, 48 h post-infection fluorescence was observed. Quantification of the number GFP-positive neurons compared to total number of neurons provided a transfection rate of close to 90% (data not shown). Besides, western blot analysis of total lysates obtained from neurons transduced with pWPI-empty vector or with pWPI-HIF-1α demonstrated that under normoxia pWPI-HIF-1α induced a very weak expression of HIF-1α protein (Fig. 6a) probably due to a rapid hydroxylation of this transcription factor by prolyl-hydroxylases and subsequent proteasome degradation. However, under hypoxia, transduction of cortical neurons with pWPI-HIF-1α significantly

increased the amount of HIF-1α stabilized compared to non-transduced and pWPI-empty vector transduced neurons exposed to hypoxia for 6h (Fig. 6a). Once determined that pWPI-HIF-1α was able to over-express HIF-1α under hypoxia the effect of this over-expression on neuronal viability was determined. Surprisingly, and contrary to what we expected, HIF-1α over-expression did not prevent hypoxia-induced neuronal death (Fig. 6b) even though silencing experiments suggested a neuroprotective role for HIF-1α.

To be certain that over expressed HIF-1α was functionally active, the expression of LDH, a well-known target protein of HIF-1α, was determined under normoxic and hypoxic conditions. Western blot analysis showed that under normoxia pWPI-HIF-1α induced an increased expression of LDH that was dependent of the volume of the stock viral utilized to transfect neurons (Fig. 6c) indicating that the protein expressed by pWPI-HIF-1α was transcriptionally active. However, under hypoxia pWPI-HIF-1α was unable to increase LDH expression further than hypoxia did (Fig. 6d), suggesting that the amount of HIF-1α stabilized by mild hypoxia was enough to reach the maximum activity of HIF-1α as transcription factor.

DISCUSSION

To maintain oxygen homeostasis, higher eukaryotes have developed specialized mechanisms to enhance oxygen uptake and distribution (Bruick, 2003). In this sense, the transcriptional complex HIF-1 plays an essential role in cellular and systemic oxygen homeostasis (Lyer et al., 1998; Semenza, 1999; Semenza, 2000). HIF-1 is a heterodimeric transcription factor composed of HIF-1α and HIF-1β subunits. Under normoxia, HIF-1α becomes ubiquinated and is rapidly degraded by the proteasome (Ivan and Kaelin, 2001;Jaakkola et al., 2001). However, under hypoxia HIF-1α is induced, stabilized, and translocates to the nucleus to regulate the transcription of a variety of genes involved in the adaptive response (Semenza, 2000). Although HIF-1α largely participates in the adaptive response during hypoxia (Sharp and Bernaudin, 2004), paradoxically it also might mediate hypoxic cell death (Carmeliet et al., 1998;Bruick, 2003;Vangeison et al., 2008). In CNS, induction and expression of HIF-1α after an ischemic insult is heterogeneous (Demougeot et al., 2004) and it has been described to play both neuroprotective and detrimental effects depending on the severity of the insult (Helton et al., 2005;Baranova et al., 2007).

The results reported here indicate that mild hypoxia (3% O_2 equivalent to a pO_2 of 22.8 mm Hg) causes a marked impairment of mitochondrial function leading to the collapse of the mitochondrial membrane potential and neuronal apoptosis by activation of the caspase-dependent intrinsic apoptotic pathway. In addition, we found that exposure of cortical neurons to mild hypoxia also induces the stabilization and translocation of HIF-1α at very initial times reaching the maximal levels of this transcription factor in the nucleus within 3 h after hypoxia. It is interesting to note that HIF-1α expression was maintained for the initial 24 hours of hypoxia, but the expression decreased after 36 h, being undetectable 48 h thereafter even if neurons

were exposed to sustained mild hypoxia for all the period of the study. This decrease in HIF-1α levels during prolonged hypoxia seems to be mediated by a decrease in its production rather by an increase in its degradation rate (Kong et al., 2007). More interestingly, the time-course of reduction in HIF-1α levels paralleled the reduction in mitochondrial function and neuronal apoptosis, suggesting a neuroprotective role for HIF-1α that disappeared when HIF-1α was degraded.

Hypoxia-induced mitochondrial ROS production, which may occur either at complex I or complex III (Semenza, 2007), might lead to a reduction in glutathione levels, the principal intracellular antioxidant system in CNS. In agreement with this, MnTBAP, a cell-permeable superoxide dismutase mimetic compound that catalyses the dismutation of superoxide radicals (Szabo, 1996;Keller et al., 1998), prevented hypoxia-induced neuronal death and increased HIF-1α protein levels in cytosol although this increase did not correlate with an increase in the amount of the transcription factor that translocated to the nucleus.

To address whether HIF-1α was playing a neuroprotective or pro-apoptotic role during mild hypoxia, we knocked down HIF-1α using shRNAi against HIF-1α mRNA introduced into neurons using a lentiviral transduction protein expression. Knocking down HIF-1α protein expression significantly potentiated hypoxia-mediated mitochondrial function impairment, depletion of GSt and mitochondrial depolarization indicating that HIF-1α plays a protective role in cortical neurons under mild hypoxia conditions. This neuroprotective effect lasted for the first 24 hours of hypoxia, but it dissapeared at longer times when HIF-1α protein levels were rapidly declining. These results agree with previous data indicating that HIF-1α also plays a protective role at very initial times in a model of chemical hypoxia in rat cortical neurons (Posadas et al., 2009) and point to a role for HIF-1α in maintaining the neuronal redox status. Supporting this view, silencing HIF-1α in a neuroblastoma cell line

increases ROS production and cell death under low oxygen levels (1% O_2) or oxygen and glucose deprivation (Guo et al., 2009).

The above results suggest that, in cortical neurons, HIF-1α prevents mild hypoxia injury mediated by ROS production for the first 24 hours. Therefore, we hypothesized that over-expression of HIF-1α would protect neurons from prolonged mild hypoxia injury. However, when cortical neurons over-expressing HIF-1α protein were exposed to mild hypoxia no beneficial effects were observed at any of the time points studied. To explain these unexpected results, we discarded that the lack of effect of HIF-1α over-expression on neuronal viability during mild hypoxia was due to the expression of an inactive transcription factor because HIF-1α increased the expression of LDH-A, a well-known target of HIF-1α (Semenza et al., 1996), during normoxia. However, LDH-A levels were not higher than those obtained by exposing the neurons to hypoxia in the absence of HIF-1α over-expression. Moreover, besides a marked enhancement of HIF-1α levels following hypoxia in neurons transduced to over-express HIF-1 α, no further increase in the expression of LDH-A was observed as compared to untreated neurons exposed to hypoxia. This might suggest that mild hypoxia stabilizes the maximal amount of HIF-1α able to act as transcription factor and to exert its neuroprotective effect. A possible explanation could be that the partner HIF-1β was acting as limiting factor in the formation of the transcription factor in the cytosol so restricting the amount of HIF-1 that translocates to the nucleus. We are currently investigating this hypothesis.

In summary, the present data suggest that HIF-1α protects neurons from death, during the initial 24 hours, following mild hypoxia, but under prolonged hypoxia this neuroprotective effect wears down and neurons eventually die by apoptosis. Moreover, our data suggest that new pharmacological approaches aimed to treat

neuronal death following hypoxia should be more effective if directed toward reducing the oxidative stress rather than to over-express HIF-1α.

References

Agius LM (2007) Complicated atheromatous plaque as integral atherogenesis. J Clin Pathol 60:589-592.

An WG, Kanekal M, Simon MC, Maltepe E, Blagosklonny MV, Neckers LM (1998) Stabilization of wild-type p53 by hypoxia-inducible factor 1alpha. Nature 392:405-408.

Baranova O, Miranda LF, Pichiule P, Dragatsis I, Johnson RS, Chavez JC (2007) Neuron-specific inactivation of the hypoxia inducible factor 1 alpha increases brain injury in a mouse model of transient focal cerebral ischemia. J Neurosci 27:6320-6332.

Bruick RK (2003) Oxygen sensing in the hypoxic response pathway: regulation of the hypoxia-inducible transcription factor. Genes Dev 17:2614-2623.

Carmeliet P, Dor Y, Herbert JM, Fukumura D, Brusselmans K, Dewerchin M, Neeman M, Bono F, Abramovitch R, Maxwell P, Koch CJ, Ratcliffe P, Moons L, Jain RK, Collen D, Keshert E (1998) Role of HIF-1alpha in hypoxia-mediated apoptosis, cell proliferation and tumour angiogenesis. Nature 394:485-490.

Cockman ME, Masson N, Mole DR, Jaakkola P, Chang GW, Clifford SC, Maher ER, Pugh CW, Ratcliffe PJ, Maxwell PH (2000) Hypoxia inducible factor-alpha binding and ubiquitylation by the von Hippel-Lindau tumor suppressor protein. J Biol Chem 275:25733-25741.

Demougeot C, Van Hoecke M, Bertrand N, Prigent-Tessier A, Mossiat C, Beley A, Marie C (2004) Cytoprotective efficacy and mechanisms of the liposoluble

iron chelator 2,2'-dipyridyl in the rat photothrombotic ischemic stroke model. J Pharmacol Exp Ther 311:1080-1087.

Ebert BL, Firth JD, Ratcliffe PJ (1995) Hypoxia and mitochondrial inhibitors regulate expression of glucose transporter-1 via distinct Cis-acting sequences. J Biol Chem 270:29083-29089.

Elbashir SM, Harborth J, Lendeckel W, Yalcin A, Weber K, Tuschl T (2001) Duplexes of 21-nucleotide RNAs mediate RNA interference in cultured mammalian cells. Nature 411:494-498.

Forsythe JA, Jiang BH, Iyer NV, Agani F, Leung SW, Koos RD, Semenza GL (1996) Activation of vascular endothelial growth factor gene transcription by hypoxia-inducible factor 1. Mol Cell Biol 16:4604-4613.

Guo S, Bragina O, Xu Y, Cao Z, Chen H, Zhou B, Morgan M, Lin Y, Jiang BH, Liu KJ, Shi H (2008) Glucose up-regulates HIF-1 alpha expression in primary cortical neurons in response to hypoxia through maintaining cellular redox status. J Neurochem 105:1849-1860.

Guo S, Miyake M, Liu KJ, Shi H (2009) Specific inhibition of hypoxia inducible factor 1 exaggerates cell injury induced by in vitro ischemia through deteriorating cellular redox environment. J Neurochem 108:1309-1321.

Halterman MW, Miller CC, Federoff HJ (1999) Hypoxia-inducible factor-1alpha mediates hypoxia-induced delayed neuronal death that involves p53. J Neurosci 19:6818-6824.

Heiss WD, Graf R (1994) The ischemic penumbra. Curr Opin Neurol 7:11-19.

Heiss WD, Graf R, Wienhard K, Lottgen J, Saito R, Fujita T, Rosner G, Wagner R (1994) Dynamic penumbra demonstrated by sequential multitracer PET after middle cerebral artery occlusion in cats. J Cereb Blood Flow Metab 14:892-902.

Helton R, Cui J, Scheel JR, Ellison JA, Ames C, Gibson C, Blouw B, Ouyang L, Dragatsis I, Zeitlin S, Johnson RS, Lipton SA, Barlow C (2005) Brain-specific knock-out of hypoxia-inducible factor-1alpha reduces rather than increases hypoxic-ischemic damage. J Neurosci 25:4099-4107.

Ivan M, Kaelin WG, Jr. (2001) The von Hippel-Lindau tumor suppressor protein. Curr Opin Genet Dev 11:27-34.

Iyer NV, Kotch LE, Agani F, Leung SW, Laughner E, Wenger RH, Gassmann M, Gearhart JD, Lawler AM, Yu AY, Semenza GL (1998) Cellular and developmental control of O2 homeostasis by hypoxia-inducible factor 1 alpha. Genes Dev 12:149-162.

Jaakkola P, Mole DR, Tian YM, Wilson MI, Gielbert J, Gaskell SJ, Kriegsheim A, Hebestreit HF, Mukherji M, Schofield CJ, Maxwell PH, Pugh CW, Ratcliffe PJ (2001) Targeting of HIF-alpha to the von Hippel-Lindau ubiquitylation complex by O2-regulated prolyl hydroxylation. Science 292:468-472.

Jordan J, Galindo MF, Calvo S, Gonzalez-Garcia C, Ceña V (2000) Veratridine induces apoptotic death in bovine chromaffin cells through superoxide production. Br J Pharmacol 130:1496-1504.

Jordan J, Galindo MF, Tornero D, Benavides A, Gonzalez C, Agapito MT, Gonzalez-Garcia C, Ceña V (2002) Superoxide anions mediate veratridine-

induced cytochrome c release and caspase activity in bovine chromaffin cells. Br J Pharmacol 137:993-1000.

Keller JN, Kindy MS, Holtsberg FW, St-Clair DK, Yen HC, Germeyer A, Steiner SM, Bruce KA, Hutchins JB, Mattson MP (1998) Mitochondrial manganese superoxide dismutase prevents neural apoptosis and reduces ischemic brain injury: suppression of peroxynitrite production, lipid peroxidation, and mitochondrial dysfunction. J Neurosci 18:687-697.

Kong X, Alvarez-Castelao B, Lin Z, Castano JG, Caro J (2007) Constitutive/hypoxic degradation of HIF-alpha proteins by the proteasome is independent of von Hippel Lindau protein ubiquitylation and the transactivation activity of the protein. J Biol Chem 282:15498-15505.

Markus R, Reutens DC, Kazui S, Read S, Wright P, Pearce DC, Tochon-Danguy HJ, Sachinidis JI, Donnan GA (2004) Hypoxic tissue in ischaemic stroke: persistence and clinical consequences of spontaneous survival. Brain 127:1427-1436.

Mukhopadhyay CK, Mazumder B, Fox PL (2000) Role of hypoxia-inducible factor-1 in transcriptional activation of ceruloplasmin by iron deficiency. J Biol Chem 275:21048-21054.

Palmer LA, Semenza GL, Stoler MH, Johns RA (1998) Hypoxia induces type II NOS gene expression in pulmonary artery endothelial cells via HIF-1. Am J Physiol 274:L212-L219.

Posadas I, Lopez-Hernandez B, Clemente MI, Jimenez JL, Ortega P, de la MJ, Gomez R, Munoz-Fernandez MA, Ceña V (2009) Highly efficient transfection of

rat cortical neurons using carbosilane dendrimers unveils a neuroprotective role for HIF-1α in early chemical hypoxia-mediated neurotoxicity. Pharm Res 26:1181-1191.

Posadas I, Santos P, Blanco A, Munoz-Fernandez M, Ceña V (2010) Acetaminophen induces apoptosis in rat cortical neurons. PLoS ONE 5:e15360.

Posadas I, Vellecco V, Santos P, Prieto-Lloret J, Ceña V (2007) Acetaminophen potentiates staurosporine-induced death in a human neuroblastoma cell line. Br J Pharmacol 150:577-585.

Ratcliffe PJ, O'Rourke JF, Maxwell PH, Pugh CW (1998) Oxygen sensing, hypoxia-inducible factor-1 and the regulation of mammalian gene expression. J Exp Biol 201:1153-1162.

Sarrafzadeh AS, Nagel A, Czabanka M, Denecke T, Vajkoczy P, Plotkin M (2010) Imaging of hypoxic-ischemic penumbra with (18)F-fluoromisonidazole PET/CT and measurement of related cerebral metabolism in aneurysmal subarachnoid hemorrhage. J Cereb Blood Flow Metab 30:36-45.

Semenza GL (1999) Perspectives on oxygen sensing. Cell 98:281-284.

Semenza GL (2000) HIF-1: mediator of physiological and pathophysiological responses to hypoxia. J Appl Physiol 88:1474-1480.

Semenza GL (2007) Oxygen-dependent regulation of mitochondrial respiration by hypoxia-inducible factor 1. Biochem J 405:1-9.

Semenza GL, Agani F, Feldser D, Iyer N, Kotch L, Laughner E, Yu A (2000) Hypoxia, HIF-1, and the pathophysiology of common human diseases. Adv Exp Med Biol 475:123-130.

Semenza GL, Jiang BH, Leung SW, Passantino R, Concordet JP, Maire P, Giallongo A (1996) Hypoxia response elements in the aldolase A, enolase 1, and lactate dehydrogenase A gene promoters contain essential binding sites for hypoxia-inducible factor 1. J Biol Chem 271:32529-32537.

Sharp FR, Bernaudin M (2004) HIF1 and oxygen sensing in the brain. Nat Rev Neurosci 5:437-448.

Shoshani T, Faerman A, Mett I, Zelin E, Tenne T, Gorodin S, Moshel Y, Elbaz S, Budanov A, Chajut A, Kalinski H, Kamer I, Rozen A, Mor O, Keshet E, Leshkowitz D, Einat P, Skaliter R, Feinstein E (2002) Identification of a novel hypoxia-inducible factor 1-responsive gene, RTP801, involved in apoptosis. Mol Cell Biol 22:2283-2293.

Siddiq A, Ayoub IA, Chavez JC, Aminova L, Shah S, LaManna JC, Patton SM, Connor JR, Cherny RA, Volitakis I, Bush AI, Langsetmo I, Seeley T, Gunzler V, Ratan RR (2005) Hypoxia-inducible factor prolyl 4-hydroxylase inhibition. A target for neuroprotection in the central nervous system. J Biol Chem 280:41732-41743.

Sowter HM, Ratcliffe PJ, Watson P, Greenberg AH, Harris AL (2001) HIF-1-dependent regulation of hypoxic induction of the cell death factors BNIP3 and NIX in human tumors. Cancer Res 61:6669-6673.

Stolze IP, Mole DR, Ratcliffe PJ (2006) Regulation of HIF: prolyl hydroxylases. Novartis Found Symp 272:15-25.

Szabo C (1996) DNA strand breakage and activation of poly-ADP ribosyltransferase: a cytotoxic pathway triggered by peroxynitrite. Free Radic Biol Med 21:855-869.

Tornero D, Posadas I, Ceña V (2011) Bcl-xL Blocks a Mitochondrial Inner Membrane Channel and Prevents Ca^{2+} Overload-Mediated Cell Death. PLoSONE 6:e20423. doi:10.1371/journal.pone.0020423.

Vangeison G, Carr D, Federoff HJ, Rempe DA (2008) The good, the bad, and the cell type-specific roles of hypoxia inducible factor-1 alpha in neurons and astrocytes. J Neurosci 28:1988-1993.

Wang GL, Semenza GL (1993) Desferrioxamine induces erythropoietin gene expression and hypoxia-inducible factor 1 DNA-binding activity: implications for models of hypoxia signal transduction. Blood 82:3610-3615.

Wiznerowicz M, Trono D (2003) Conditional suppression of cellular genes: lentivirus vector-mediated drug-inducible RNA interference. J Virol 77:8957-8961.

Wiznerowicz M, Trono D (2005) Harnessing HIV for therapy, basic research and biotechnology. Trends Biotechnol 23:42-47.

Wood KA, Youle RJ (1995) The role of free radicals and p53 in neuron apoptosis in vivo. J Neurosci 15:5851-5857.

LEGENDS.

Figure 1. **Lost of neuronal death induced by mild hypoxia is mediated by activation of the intrinsic cell death pathway. a**) Time-course of cortical neurons viability under hypoxia (Hx) expressed as the percentage of MTT transformed related to normoxia (Nx). Data are expressed as mean ± SEM of 12 experiments, n=12. **p<0.01, ***p<0.001, as compared to neurons exposed to normoxia (Nx). b) Representative images of cortical neuronas exposed to either normoxia (Nx) or hypoxia (Hx) for 24 hours and stained with Hoescht 33342. Arrowheads indicate condensed nuclei and chromatin fragmentation. Images are representative of three independent experiments. c) Time-course of the effect of hypoxia (Hx) on cytochrome c (Cyt C) release from mitochondria to cytosol. Graphs represent densitometric analysis of Cyt C normalized to α-tubulin as protein loading control in cytosolic fractions (upper panel, right image), and densitometric analysis of Cyt C normalized to COXIV as protein loading control in mitochondrial fractions (lower panel, right image). Data are expressed as mean ± SEM of 3 experiments. **p<0.01, ***p<0.001 as compared to neurons exposed to normoxia (Nx). d) Time-course of caspase 3 activation induced by hypoxia (Hx) in rat cortical neurons. Data are expressed as mean ± SEM of 12 experiments. *p<0.05, ***p<0.001 as compared to neurons exposed to normoxia (Nx).

Figure 2. **Hypoxia induces HIF-1α protein stabilization and translocation to the nucleus.** a) Time-course of HIF-1α expression in total lysates of rat cortical neurons after exposure to hypoxia (Hx). Graph represents densitometric analysis of HIF-1α protein levels normalized to α-tubulin as protein loading control. Data are expressed as mean ± SEM of 3 experiments. *p<0.05, ***p<0.001 as compared to neurons incubated under normoxia (Nx). **b**) Upper panel. Time-course of HIF-1α expression

in cytosolic fractions obtained from cortical neurons exposed to hypoxia (Hx) for different times. Graph represents densitometric analysis of HIF-1α protein levels normalized to α-tubulin as cytosolic protein loading control. Data are expressed as mean ± SEM of 3 experiments. *p<0.05, ***p<0.001 as compared to neurons incubated under normoxia (Nx). Lower panel. Time-course of HIF-1α expression in nuclear fractions obtained from cortical neurons exposed to hypoxia (Hx) for different times. Graph represents densitometric analysis of HIF-1α protein levels normalized to Histone 2A (H2A) as nuclear protein loading control. Data are expressed as mean ± SEM of 3 experiments. ***p<0.001 as compared to neurons incubated under normoxia (Nx).

Figure 3. Oxidative stress plays a central role in mild hypoxia-induced neuronal death. a) Time-course of mitochondrial superoxide production under hypoxia condition. Left column: Hoeschst staining of cortical neuron nuclei incubated with normoxia (Nx) or hypoxia (Hx) for different times; Middle column: Fluorescence images of rat cortical neurons exposed to normoxia (Nx) or hypoxia (Hx) for different times and then loaded with Mitosox probe; Right column: Merged images of Hoeschst staining and fluorescent Mitosox pannels are shown. b) Time-course of hypoxia-induced reduction of total glutathione neuronal levels, expressed as percentage of glutathione related to normoxic levels (% GSt). Data are expressed as mean ± SEM of 3 experiments.**p<0.01; ***p<0.001 as compared to cells incubated under normoxia. c) Effect of hypoxia on mithochondrial transmembrane potential (Ψm), expressed as percentage of Ψm related to that observed under normoxia. Data are expressed as mean ± SEM of 3 experiments.*p<0.05; **p<0.01; ***p<0.001 as compared to cells incubated under normoxia. **d)** Effect of MnTBAP on

hypoxia-induced neuronal death. Data are expressed as mean ± SEM of 3 experiments.***p<0.001 as compared to neurons exposed to normoxia.

Fig 4. **Lentiviral-mediated introduction of RNAi into primary neurons leads to efficient transduction and complete silencing of HIF-1α expression.** a) Left column: bright field (bf) of cortical neurons transduced with a control lentivirus vector expressing a random sequence (shR) or lentivirus vector expressing a short hairpin sequence that produce a small interfering RNA directed against HIF-1α mRNA (shH); middle column: GFP expression in cortical neurons transduced with shR and shH; right column: merged images of rat cortical neurons transduced with each lentivirus 24 hours after exposure. b) Effect of shR and shH on HIF-1α protein levels detected on total lysates obtained from cortical neurons exposed to normoxia (Nx) hypoxia condition for 6 hours (Hx 6h). Graph shows densitometric analysis of of HIF-1α protein levels normalized to α-tubulin as protein loading control. Data are expressed as mean ± SEM of 3 experiments. ***p<0.001 as compared to neurons incubated under normoxia (Nx).

Fig 5. **HIF-1α knocking down increases the deleterious effect of hypoxia on cortical neurons.** a) Effect of HIF-1α knocking down on mithochondrial transmembrane potential (Ψm) under hypoxia. Rat cortical neurons were transduced with pLVTHM-shR (shR) or pLVTHM-shH (shH) for 24 hours and then incubated under normoxia (Nx) or hypoxia (Hx) for 18h. Changes in Ψm are expressed as the percentage of Ψm under normoxic conditions. Data are expressed as mean ± SEM of 3 experiments.***p<0.001 as compared to cells incubated under hypoxia. b) Left panel: Cyt C protein levels in cytosolic fractions obtained from cortical neurons transduced with shR or shH and exposed to normoxia (Nx) or hypoxia (Hx) for 18 h.

Graph represents densitometric analysis of HIF-1α protein levels normalized to α-tubulin as cytosolic protein loading control. Data are expressed as mean ± SEM of 3 experiments. ***p<0.001 as compared to neurons incubated under normoxia (Nx). Right panel: Cyt C protein levels in mitochondrial fractions obtained from cortical neurons transduced with shR or shH and exposed to normoxia (Nx) or hypoxia (Hx) for 18 h. Graph represents densitometric analysis of Cyt C protein levels normalized to COX-IV as mitochondrial protein loading control. protein levels. c) Caspase 3 activity measured in total lysates obtained from cortical neurons transduced with shR or shH and exposed to normoxia (Nx) or hypoxia (Hx) for 24 h. Data are expressed as mean ± SEM of 12 experiments. ***p<0.001 as compared to cells incubated under normoxia . ≈≈≈P<0.001 as compared with hypoxia alone. d) Effect of HIF-1α silencing expression on hypoxia induced-GSt depletion. (○) GSt levels under normoxia, (●) GSt levels under hypoxia, (◆) GSt levels in shR-transduced cortical neurons under hypoxia, (■) GSt levels in shH-transduced cortical neurons under hypoxia. Data are expressed as mean ± SEM of 3 experiments. ***p<0.001 compared to hypoxia-treated group. e) Time-course of the effect of pLVTHM-shR (shR) (◇,◆, normoxia and hypoxia respectively) or pLVTHM-shH (shH) (□, ■, normoxia and hypoxia respectively) transduction under normoxic (○) or hypoxic (●) conditions on rat cortical neurons survival. Cortical neurons were transduced with the corresponding lentiviral vectors and the viability was evaluated measuring the percentage of MTT transformed under normoxia or hypoxia for different times. Data are expressed as mean ± SEM of 12 experiments .*p<0.05; **p<0.01; ***p<0.001 as compared to cells incubated under normoxia.

Fig 6. **Effect of lentivirus-mediated transgene overexpression of HIF-1α on hypoxia-induced neuronal death**. a) HIF-1α protein levels detected in total lysates of cortical neurons transduced with pWPI-HIF-1α (pWPI-H), for transgene expression of HIF-1α, or control vector, (pWPI-C) and exposed to normoxia (Nx 6h) or hypoxia for 6 h (Hx 6h). Graph represents densitometric analysis of HIF-1α protein levels normalized to α-tubulin (α –tub) as protein loading control. Data are expressed as mean ± SEM of 3 experiments . ***p<0.001 as compared to cells incubated under hypoxia. b) Time-course of the effect of pWPI-C (◇,◆, normoxia and hypoxia respectively) or pWPI-H (□, ■, normoxia and hypoxia respectively) transduction under normoxic (○) or hypoxic (●) conditions. Cortical neurons were transduced with the corresponding lentiviral vectors and the viability was evaluated measuring the percentage of MTT transformed under normoxia or hypoxia for different times. Data are expressed as mean ± SEM of 12 experiments. c) LDHA expression detected in total lysates obtained from cortical neurons transduced with different volumes of pWPI-C (Nx-E) or pWPI-H (Nx-H) under normoxia. Graph represents densitometric analysis of HIF-1α protein levels normalized to α-tubulin (α –tub) as protein loading control. Data are expressed as mean ± SEM of 3experiments .***p<0.001 as compared to non-transduced cells (Nx). d) LDHA expression detected in total lysates obtained from cortical neurons transduced with different volumes of pWPI-C (Hx-E) or pWPI-H (Hx-H) under hypoxia. Graph represents densitometric analysis of HIF-1α protein levels normalized to α-tubulin (α –tub) as protein loading control. Data are expressed as mean ± SEM of 3 experiments .***p<0.001 compared with non-transduced cells (Hx).

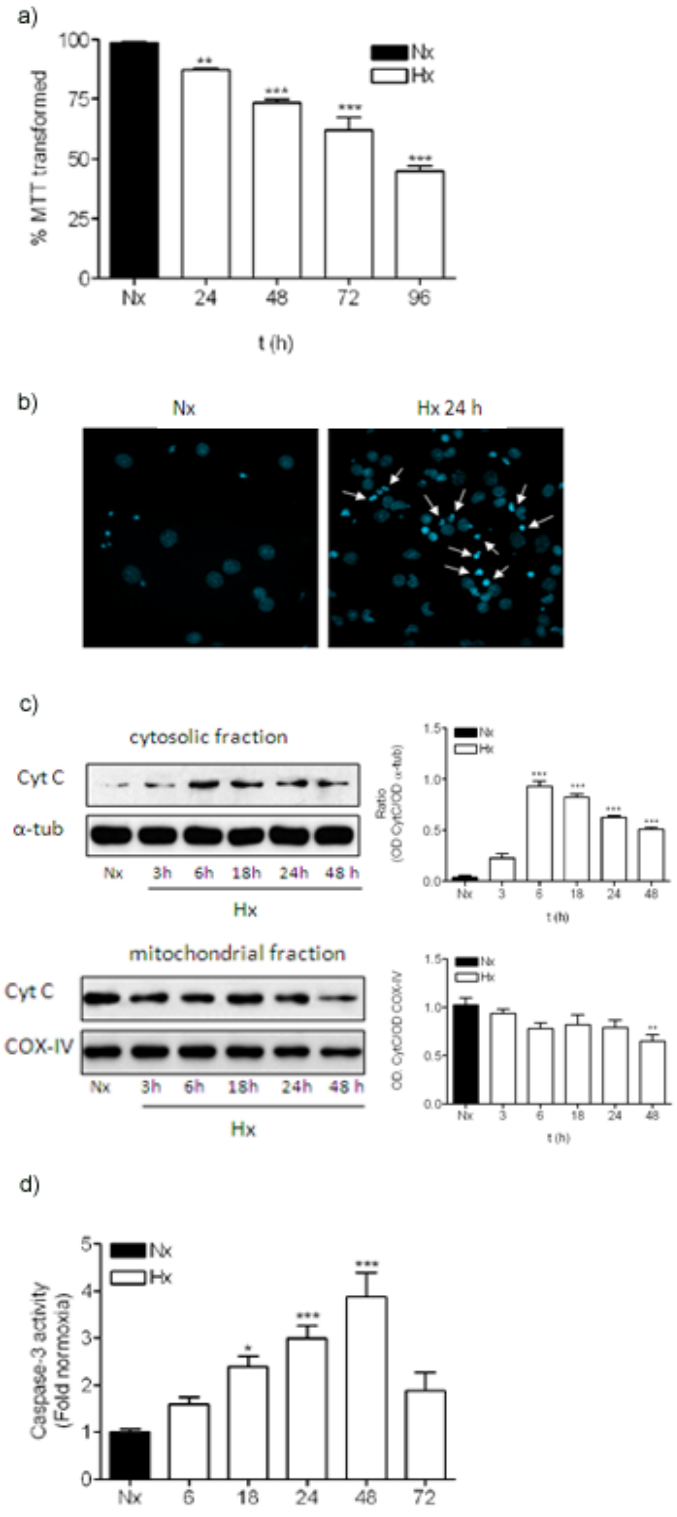
a)
% MTT transformed
Nx
Hx
t (h)
b)
Nx
Hx 24 h
c)
cytosolic fraction
Cyt C
α-tub
Nx 3h 6h 18h 24h 48 h
Hx
mitochondrial fraction
COX-IV
d)
Caspase-3 activity (Fold normoxia)

Figure 1

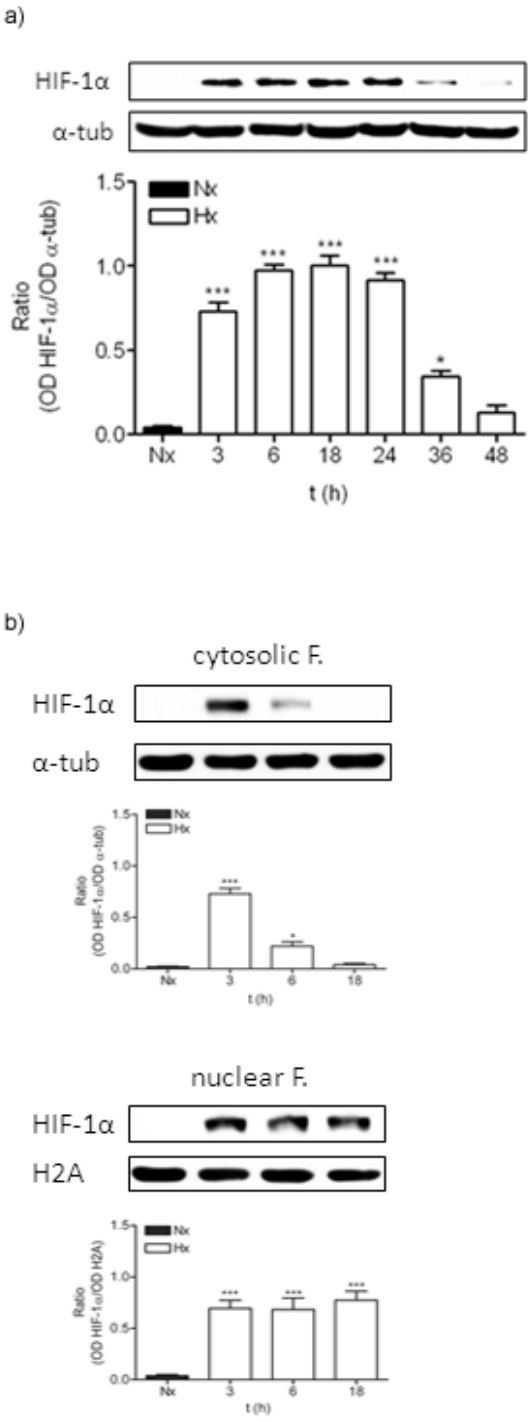
a)
HIF-1α
α-tub
Nx
Hx
Ratio (OD HIF-1α/OD α-tub)
1.5
1.0
0.5
0.0
***
***
***
***
*
Nx
3
6
18
24
36
48
t (h)
b)
cytosolic F.
HIF-1α
α-tub
Nx
Hx
Ratio (OD HIF-1α/OD α-tub)
***
*
Nx
3
6
18
t (h)
nuclear F.
HIF-1α
H2A
Nx
Hx
Ratio (OD HIF-1α/OD H2A)
***
***
***
Nx
3
6
18
t (h)

Figure 2

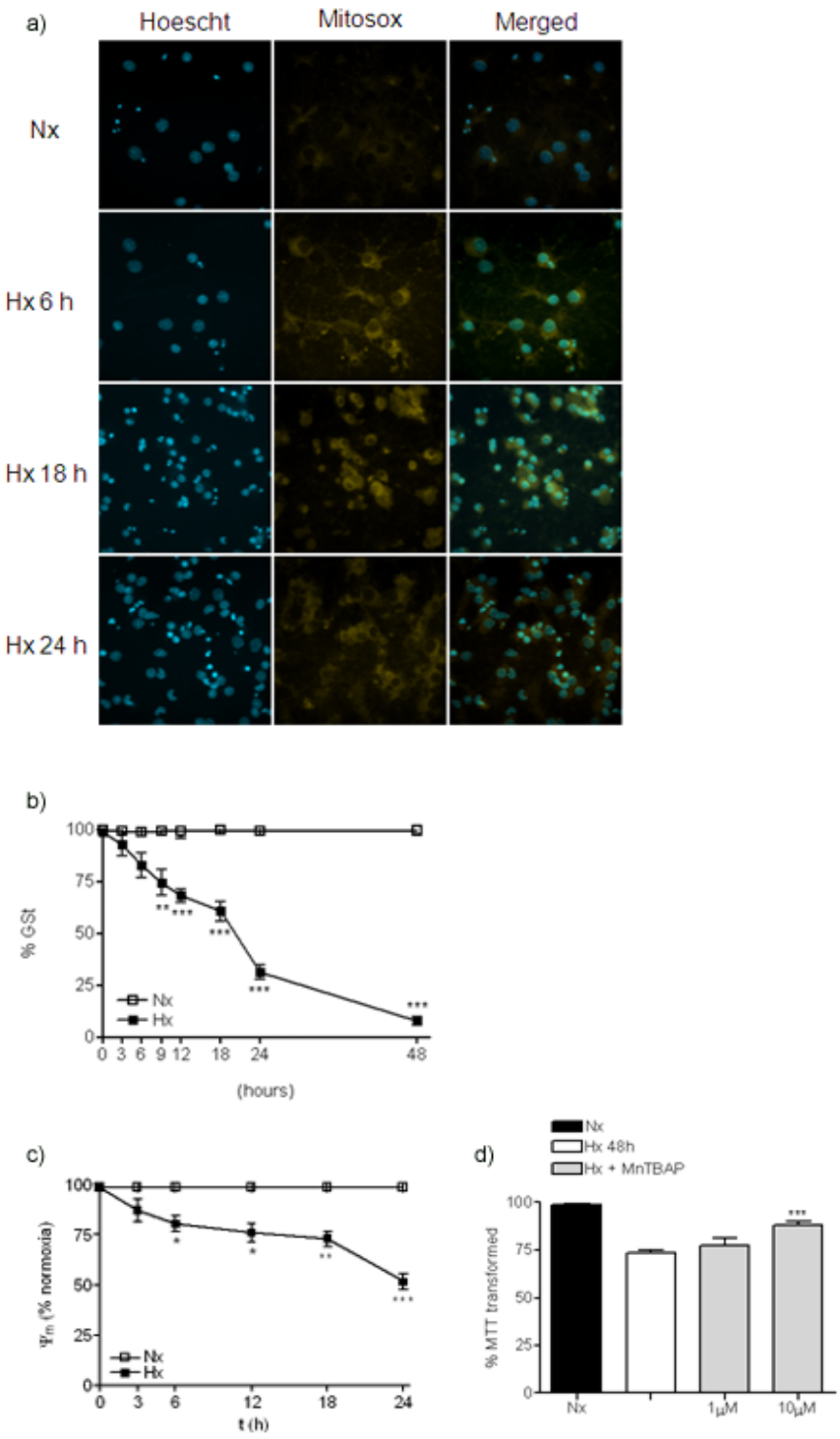
a)
Hoescht
Mitosox
Merged
Nx
Hx 6 h
Hx 18 h
Hx 24 h
b)
% GSt
100
75
50
25
0
0 3 6 9 12 18 24 48
(hours)
Nx
Hx
c)
Ψm (% normoxia)
100
75
50
25
0
0 3 6 12 18 24
t (h)
Nx
Hx
d)
Nx
Hx 48h
Hx + MnTBAP
% MTT transformed
100
75
50
25
0
Nx
1μM
10μM

Figure 3

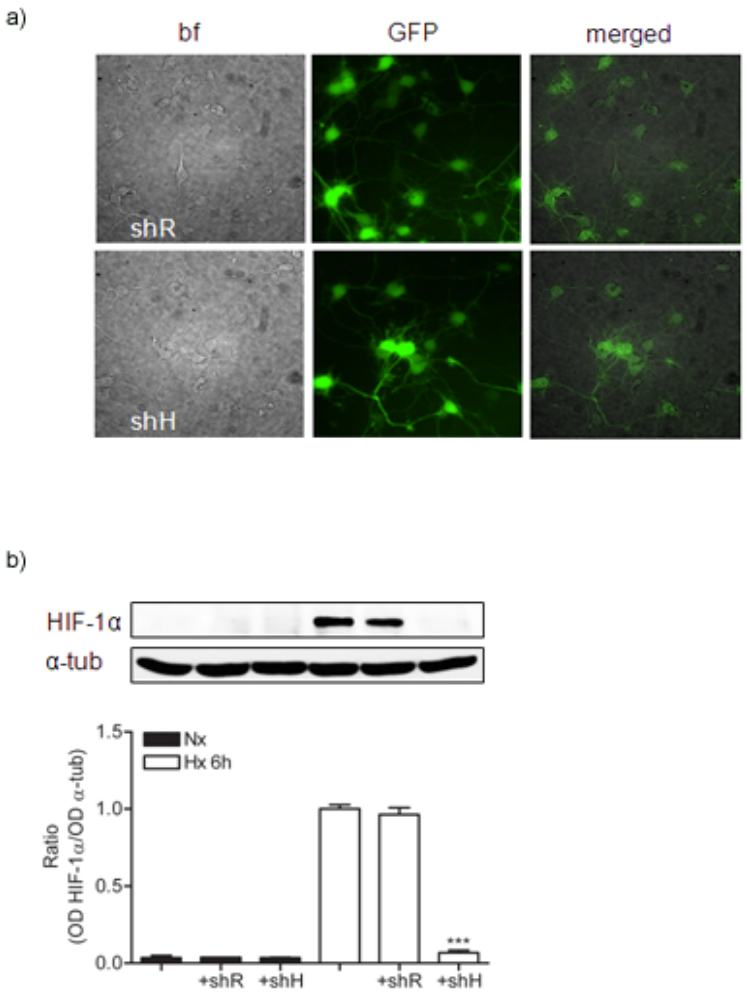
a)
bf
GFP
merged
shR
shH
b)
HIF-1α
α-tub
Nx
Hx 6h
Ratio
(OD HIF-1α/OD α-tub)
1.5
1.0
0.5
0.0
***
+shR
+shH
+shR
+shH

Figure 4

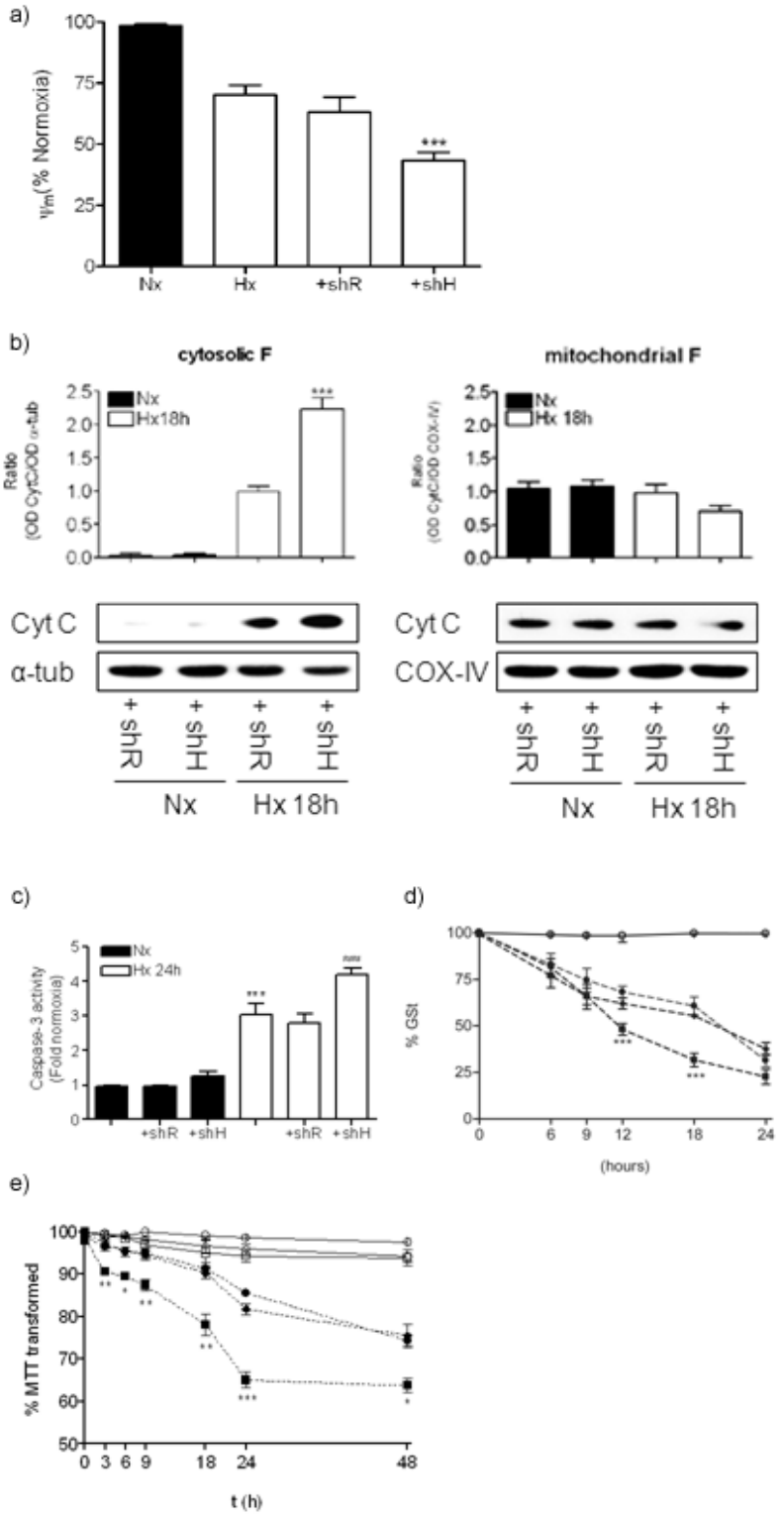
a)
100
75
50
25
0
Ψm (% Normoxia)
***
Nx
Hx
+shR
+shH
b)
cytosolic F
mitochondrial F
Nx
Hx18h
Hx 18h
Ratio (OD CytC/OD α-tub
Ratio (OD CytC/OD COX-IV)
***
Cyt C
α-tub
COX-IV
+ shR
+ shH
Nx
Hx 18h
c)
Nx
Hx 24h
Caspase-3 activity (Fold normoxia)
***
+shR
+shH
d)
% GSI
(hours)
e)
% MTT transformed
t (h)

Figure 5

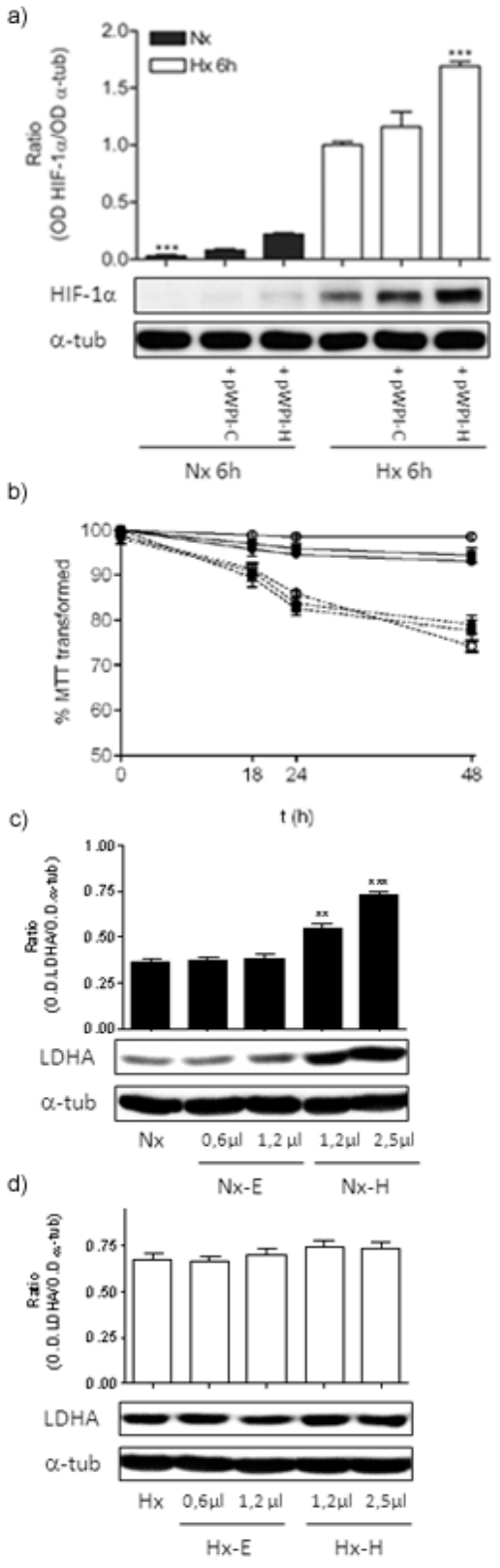
a)
Nx
Hx 6h
Ratio (OD HIF-1α/OD α-tub)
2.0
1.5
1.0
0.5
0.0
***
***
HIF-1α
α-tub
+PMPI-C
+PMPI-H
+PMPI-C
+PMPI-H
Nx 6h
Hx 6h
b)
% MTT transformed
100
90
80
70
60
50
0
18
24
48
t (h)
c)
Ratio (O.D.LDHA/O.D.α-tub)
1.00
0.75
0.50
0.25
0.00
**
***
LDHA
α-tub
Nx
0,6µl
1,2 µl
1,2µl
2,5µl
Nx-E
Nx-H
d)
Ratio (O.D.LDHA/O.D.α-tub)
0.75
0.50
0.25
0.00
LDHA
α-tub
Hx
0,6µl
1,2 µl
1,2µl
2,5µl
Hx-E
Hx-H

Figure 6